DOI 10.1002/prot.24540

Talin-driven inside-out activation mechanism of platelet αIIbβ3 integrin probed by multi-microsecond, all-atom molecular dynamics simulations

Davide Provasi[1,†], Ana Negri[1,†], Barry S. Coller[2], and Marta Filizola[1,*]

[1]Department of Structural and Chemical Biology, Icahn School of Medicine at Mount Sinai, One Gustave L. Levy Place, Box 1677, New York, NY 10029; [2]Allen and Frances Adler Laboratory of Blood and Vascular Biology, The Rockefeller University, 1230 York Avenue, Box 309, New York, NY 10065.

[†] These authors contributed equally to this study.

[*]To whom correspondence should be addressed:

Dr. Marta Filizola

Department of Structural and Chemical Biology

Icahn School of Medicine at Mount Sinai

One Gustave L. Levy Place, Box 1677; New York, NY 10029-6574

Tel: 212-659-8690; Fax: 212-849-2456; Email: marta.filizola@mssm.edu

Short title: Long-scale MD of the integrin-talin complex

Keywords: Anton, long-scale MD, molecular complex, membrane, CHARMM

Received: Nov 15, 2013; Revised: Feb 06, 2014; Accepted: Feb 10, 2014

ABSTRACT

Platelet aggregation is the consequence of the binding of extracellular bivalent ligands such as fibrinogen and von Willebrand factor to the high affinity, active state of integrin αIIbβ3. This state is achieved through a so-called "inside-out" mechanism characterized by the membrane-assisted formation of a complex between the F2 and F3 subdomains of intracellular protein talin and the integrin β3 tail. Here, we present the results of multi-microsecond, all-atom molecular dynamics simulations carried on the complete transmembrane (TM) and C-terminal (CT) domains of αIIbβ3 integrin in an explicit lipid-water environment, and in the presence or absence of the talin-1 F2 and F3 subdomains. These large-scale simulations provide unprecedented molecular-level insights into the talin-driven inside-out activation of αIIbβ3 integrin. Specifically, they suggest a preferred conformation of the complete αIIbβ3 TM/CT domains in a lipid-water environment, and testable hypotheses of key intermolecular interactions between αIIbβ3 integrin and the F2/F3 domains of talin-1. Notably, not only do these simulations give support to a stable left-handed reverse turn conformation of the αIIb juxtamembrane motif rather than a helical turn, but they raise the question as to whether TM helix separation is required for talin-driven integrin activation.

INTRODUCTION

Integrin αIIbβ3 is a hetero-dimeric receptor complex that mediates platelet aggregation through binding extracellular bivalent ligands such as fibrinogen and von Willebrand factor.[1] Each subunit of this complex features a large extracellular domain (ECD), a single-spanning transmembrane (TM) helix, and an intracellular cytoplasmic tail (CT). The heterodimer normally resides in the low-affinity resting state on the cell surface (or bent conformation as shown by X-ray crystallography and electron microscopy[2]), and can transmit bi-directional signals across the cell membrane via inside-out and outside-in pathways.[3,4] The former is activated upon interaction of intracellular proteins such as talin and kindlin with residues of the integrin β3 CT domain, and results in long-range propagation of conformational changes to the integrin ECD,[5,6] leading to the receptor adopting a high affinity state for its extracellular ligands.[7] This high affinity state is believed to feature an extended and "swung-out" (open) conformation of the ECD,[8,9] as well as separated TMs.[10-17] However, recent studies of intact αIIbβ3 using solution X-ray scattering and electron microscopy[18] have challenged the well-established idea of TM domain separation[10-17] given that the C-terminal portions of the αIIb and β3 subunits and the legs were seen to be close together in all detected conformations of the protein, including bent, extended-closed, or extended-open conformations. Moreover, the addition of talin head domain to purified αIIbβ3 embedded in a DMPC/DMPG lipid bilayer nanodisc in the absence of detergent resulted in extension of the receptor and enhanced ligand binding, but not leg separation.[5] Thus, there is controversy as to whether integrin TM domain separation is necessary for integrin activation under physiologic conditions. Since activation of the αIIbβ3 receptor is required to achieve hemostasis, but may lead to harmful thrombus formation and consequent ischemic arterial diseases, understanding how, at the molecular level, "inside-out" signaling

propagates from the site of interaction between cellular activators and the receptor CTs to the TM dimer, and ultimately to the ECD, has important clinical implications.

A wealth of recent experimental[19-24] and computational[25-28] studies has unveiled important details of the molecular mechanism underlying integrin inside-out activation. However, these insights have mostly been inferred from incomplete or isolated αIIbβ3 integrin TM/CT constructs, short all-atom simulations, or serial multiscale approaches combining coarse-grained simulations of membrane association with atomistic refinements. In the present study, we carried out all-atom, multi-microsecond molecular dynamics (MD) simulations of the complete αIIbβ3 integrin TM/CT domains in an explicit lipid-water environment, and with the αIIb juxtamembrane motif in either a helical or left-handed reverse turn conformations, as observed by NMR in an organic-water mixture[21] or phospholipid bicelles,[29] respectively. The system with a left-handed reverse turn conformation of the αIIb juxtamembrane motif was the only one to remain stable during microsecond-scale MD simulations, and was then also simulated in the presence of the talin-1 F2-F3 domains using the massively parallel special-purpose supercomputer Anton[30] for MD simulations. Results of these simulations provide an unprecedented level of molecular detail on the conformational dynamics that promote transition of αIIbβ3 to its high affinity state.

MATERIAL AND METHODS

System setups

Initial molecular models of the complete αIIbβ3 integrin TM/CT domains (Fig. 1), including linkers between the TMs and ECD, specifically residues αIIb A958-E1008/β3 P685-T762, with

the αIIb juxtamembrane segment 991GFFKR995 in either a helical or left-handed reverse turn conformation were built using as structural templates NMR structures corresponding to PDB codes 2KNC (αIIb G955-E1008/β3 G684-T762)[21] or 2K9J (αIIb G957-P998/β3 P685-F727),[29] respectively. Specifically, the model with a helical αIIb 991GFFKR995 segment was based entirely on the 2KNC structure, whereas in the model with this segment in a left-handed reverse turn conformation, missing parts of the 2K9J structure (αIIb P998- E1008, β3 F727-A750, and β3 T751-T762) were taken from 2KNC, a β3 model based on the crystal structure of the integrin β1D CT domain in complex with murine talin-2 F2-F3 (PDB: 3G9W[31]), and the NMR structure of the complete β3 CT domain (PDB: 2KV9[22]), respectively. A complex of this latter complete αIIbβ3 TM/CT model with talin-1 F2-F3 (residues S206-S405) was generated on the basis of the crystal structure corresponding to PDB code 3G9W,[31] using the integrin β1D CT domain in complex with the highly homologous murine talin-2 as structural templates for the corresponding β3 and talin-1 domains, respectively. Residues that had been mutated in the experimental constructs were replaced by corresponding amino acids in normal human αIIbβ3 sequences.

Atomistic MD simulations

The 2KNC-based and 2K9J-based systems without talin and the 2K9J-based model with talin were embedded into pre-equilibrated, TIP3P-hydrated 1-palmitoyl-2-oleoyl-sn-glycero-3-phospho-choline (POPC) lipid patches of 81×78×129 Å, taking into consideration the suggested perpendicular orientation of the αIIb TM helix to the plane of the membrane,[29,32] and the need for a positively charged patch of the talin F2 domain to face the membrane.[31] The resulting systems in the presence or absence of talin were neutralized by 8 Cl^- or 3 Na^+ counter-ions, and arranged in unit cells of 79×76×124 $Å^3$ or 53×81×124 $Å^3$ containing ~76,000 or ~50,000 atoms,

respectively. The CHARMM27 force field topology and parameters[33] with the CMAP backbone energy correction[34] were used to describe these systems. Following energy minimization and 50 ns equilibration runs with Desmond 2.4, standard, unrestrained MD production simulations were carried out using the NPT ensemble controlled using the Berendsen thermostat and barostat at 300 K and 1 atm, respectively, as well as reversible reference system propagator algorithms (RESPA) with a timestep of 2.0 fs for both the bonded and the near non-bonded interactions and of 6.0 fs for the far non-bonded interactions. The 2KNC-based and 2K9J-based systems without talin were simulated for ~4.0 and ~3.0 μs, respectively, whereas the 2K9J-based complex with talin was simulated for ~5.0 μs. Most simulations were carried out on the special-purpose supercomputer Anton.[30]

Analyses of MD simulations

Simulations were analyzed using various tools, including in-house R scripts to measure crossing and tilting angles of the TM helices, as well as the fraction of intramolecular HN-NH restraints used to obtain the 2KNC and 2K9J NMR ensembles. Gromacs tools g_energy and g_dist were used to calculate interaction energies and inter-atomic distances, respectively. Rotation and bending of the TM helices were calculated with the TRAJELIX module[35] of the SIMULAID package.[36] Briefly, after superposition of the helix axis to the axis of the reference structure, the angle between the vectors projecting the Calpha atom on the helix axis in each frame were calculated for each residue, and its increment averaged over the whole TM region to yield the mean rotation angle. All time-course plots report averages obtained using a moving linear filter with a 100 ns bandwidth, superimposed to raw data sampled with a 1 ns frequency, as well as boxplots indicating the average, the 1st and 3rd quartiles, and 1.5 interquartile range whiskers.

RESULTS AND DISCUSSION

The αIIbβ3 TM/CT structure with a helical juxtamembrane segment (2KNC) is unstable in an explicit lipid-water environment.

Two experimental model structures have been reported in the literature for the αIIbβ3 TM/CT domain: a) an NMR structure (PDBid: 2KNC)[21] of the complete integrin αIIbβ3 TM and CT domains (αIIb E960-E1008/β3 K689-T762) in a CD3CN/H2O mixture (Fig. 1A), and b) an NMR structure (PDB: 2K9J)[29] of the same complex with truncated CT domains (αIIb A958-P998/β3 P685-F727) in phospholipid bicelles (Fig. 1B). Both model structures are characterized by a right-handed crossing angle between the αIIb and β3 subunits (–22˚, –32˚ in 2K9J and 2KNC, respectively), and by two main sites of inter-subunit interaction: the so-called outer membrane and inner membrane clasps (or OMC and IMC, respectively). Unlike the OMC (Fig. 1C/1D), which is characterized by packing interactions between glycines of the αIIb 972GXXXG976 motif and β3 V700/M701/I704 residues, as well as between αIIb L979/ L980 and β3 L705/G708 residues, the IMC (Fig. 1E/1F), which includes residues of the highly conserved αIIb juxtamembrane 991GFFKR995 motif, differs significantly between the two NMR structures of the αIIbβ3 TM/CT domains. Specifically, while the αIIb 991GFFKR995 motif exhibits a left-handed reverse turn in lipid bicelles (2K9J[29] or Fig. 1B), it rather assumes a helical conformation in the CD3CN/H2O mixture (2KNC[21] or Fig. 1A). Notably, the left-handed reverse turn was predicted to be the most stable conformation of the αIIb 991GFFKR995 segment by a Rosetta Membrane[37,38] computational model generated using disulfide-based distance restraints inferred from experiments of intact integrins on the cell surface.[39] In both the NMR structure in lipid bicelles (2K9J)[29] and the Rosetta model[39] this conformation placed both

αIIb F992/F993 side chains inside the membrane at the interface between the αIIb and β3 subunits (Figure 1F), allowing them to form interactions with αIIb M987 and β3 L712/W715/K716/I719. In contrast, in the NMR structure obtained in the CD3CN/H2O mixture (2KNC)[21] the αIIb F992/F993 side chains were not found at the interface between the αIIb and β3 subunits, and the IMC (Fig. 1E) appeared to be stabilized by a weak interaction between αIIb 990VGF992 and β3 I719.

A common feature of the IMC in the two different NMR structures[21,29] is a salt bridge between αIIb R995 and β3 D723 (Fig. 1E/1F). Conflicting experimental evidence exists in the literature regarding the ability of this salt-bridge to stabilize an inactive αIIbβ3 conformation. Early experiments in stable CHO transfectants using alanine mutations and 'charge-reversal' mutations of the αIIb R995 and β3 D723 residues suggested a role for each member of this salt bridge in keeping the receptor in a resting state, although mutating D723 to alanine produced more activation than mutating it to arginine.[40] In addition, NMR experiments in aqueous conditions demonstrated that an αIIb R995D mutation disrupted the interaction between peptides comprising the αIIb tail (K989-E1008) and the β3 tail (K716-T762), as did the addition of talin.[41] Later experiments in both 293T transfectants and transient CHO-K1 cells,[39] however, showed minimal activation by a β3 D723A mutation. Interpreting the results of β3 D723 mutations is potentially confounded by the suggestion that β3 D723 participates in the activation process through a direct interaction with talin-1 K324.[31] In view of the above evidence supporting a role for the αIIb R995-β3 D723 interaction in maintaining αIIbβ3 in a low affinity state, it was surprising that the αIIb R995 and β3 D723 side chains were within hydrogen-bonding distance in only 16% of the low energy structures identified by Rosetta modeling.[39] This study noted that αIIb R995 and β3 D723 both sample a large conformational space and that the

R995 side chain can also interact with β3 D726, creating an alternative salt bridge to maintain the receptor in an inactive conformation.

In contrast to the relatively low frequency of αIIb R995-β3 D723 interactions identified in the Rosetta conformation sampling, interactions between the β3 K716 side chain and the αIIb F992/K994 backbone carbonyl oxygens were recorded in 65% of the structures in the Rosetta conformational sampling, and the functional role of this interaction was supported by demonstrating that mutating β3 K716 to any other residue led to the integrin adopting a high-affinity state.[39] However, the interactions between β3 K716 and αIIb F992/K994 backbone carbonyl oxygens are missing in both NMR structures, although the β3 K716 side chain was found in the vicinity of the αIIb M987 backbone carbonyl oxygen in the NMR structure obtained in the CD3CN/H2O mixture (2KNC[21]).

A multi-step inside-out signaling mechanism was proposed[21] to reconcile the differences between the two existing NMR structures of the αIIbβ3 TM/CT domains.[21,29,39] According to this proposal, the αIIb juxtamembrane helical motif of 2KNC corresponds to a native conformation in the aqueous cytoplasm that transitions into an intermediate, transient state represented by the alternative left-handed reverse turn conformation of 2K9J along the integrin activation pathway. To investigate the likelihood of these NMR model structures in an explicit lipid bilayer, we carried out multi-microsecond, unrestrained MD simulations of complete αIIbβ3 TM/CT models (see Fig. 1A/1B) built in an explicit, hydrated lipid bilayer following the procedure described in Materials and Methods.

Our extended, 4 μs all-atom simulations of the 2KNC-based model structure with an αIIb 991GFFKR995 helical segment (Fig. 1A) reveal helix unwinding after ~2 μs in an explicit lipid-water environment, and embedding of both αIIb F992/F993 aromatic rings into the membrane.

This observation suggests instability of the 2KNC-based structure in a lipid bilayer as demonstrated by an increased RMSD from the 2KNC experimental structure and a slightly decreased one from the 2K9J structure (see Fig. S1A). Notably, ~70% and ~85% of the NOE distance restraints are satisfied for αIIb and β3 respectively during simulation of both systems.

The 2KNC is also notable for the αIIb F992, but not the F993, aromatic ring positioning itself between the αIIb and β3 subunits, thus establishing interactions with β3 L712/W715 during the simulated timescale. The salt-bridge interaction between αIIb R995 and β3 D723 is relatively unstable during the first 2.5 μs of these simulations, but then stabilizes during the remainder of the simulation time (see Fig. S3A). Notably, no additional interactions of β3 K716 with the αIIb F992/K994 backbone carbonyl oxygens were observed in these simulations (see Fig. S3B and 3C).

Unlike the 2KNC-based structure, the 2K9J-based complete αIIbβ3 TM/CT model structure is very stable during the achieved 3 μs MD simulations, maintaining a small RMSD from the initial conformation (Fig. S1B), as well as the main interactions within IMC and OMC. Not only does the left-handed reverse turn of the αIIb 991GFFKR995 segment remain unaltered during these simulations (with an average backbone root mean square deviation of 0.84 Å with respect to the initial conformation), as also inferred from Rosetta modeling,[39] but the IMC interactions between the αIIb F992/F993 side chains and αIIb M987 or β3 L712/W715/K716/I719 are mostly preserved (see time evolution of these interactions in Fig. S4A) throughout the simulated timescale. This is also the case for the OMC interactions between αIIb G972/G976/L979/L980 and β3 V700/M701/I704/L705/G708 (Fig. S4B), given that the right-handed crossing angle between the αIIb and β3 TM helices remains mostly confined to a $-33^{\circ}\pm8^{\circ}$ value during simulation (black line in Fig. 2A). This angle was reported to be -32°,

−22˚, −37˚, or −35˚ in the two structures obtained by NMR,[21,29] the experimentally-driven Rosetta modeling,[39] and recent multiscale MD simulations,[26] respectively.

Whereas the Rosetta modeling indicated that only a small percentage of low energy structures exhibit the IMC salt-bridge interaction between αIIb R995 and β3 D723, our simulations of the complete αIIbβ3 integrin TM/CT domains in an explicit lipid bilayer show a stable αIIb R995-β3 D723 interaction with, or without, talin during the simulated timescale (black line in Fig. 4A). While our data are consistent with this salt bridge playing an important role in maintaining the receptor in the resting state, as discussed above, data on the importance of this salt bridge are complex and difficult to reconcile.[10,21,31,40,41] Similarly, while functional studies of the talin K324D mutant, which was designed on the basis of an overlay of the talin2/β1D structure,[31] suggest that talin disrupts the αIIbβ3 TM structure by interacting with β3 D723 and disrupting the latter's interaction with αIIb R995,[29] we did not observe competition of talin-1 with the αIIb R995-β3 D723 interaction during the simulated timescale. We cannot, of course, exclude the possibility that we would have observed such competition if we performed longer simulations.

Our simulations confirm the formation of new, mostly stable interactions between the β3 K716 side chain and the αIIb F992/K994 backbone carbonyl oxygens (black lines in Fig. 3B and 3C, respectively) as seen in 65% of structures sampled by Rosetta.[39] These findings further support the proposed functional role of β3 K716 based on the observation that its mutation to any other residue leads to the integrin adopting a high-affinity state.[39]

Since the long simulations of the complete αIIbβ3 TM/CT domain support a stable 2K9J-based model structure in a lipid bilayer, we chose this model to study the system in the presence of talin (Fig. 4).

The αIIb TM helix does not remain perpendicular to the plane of the membrane.

Several different experiments have been carried out to infer the location of the αIIbβ3 TM helices in the membrane. Early glycosylation mapping in a cell-free system[42,43] and NMR structures of the isolated αIIb and β3 subunits in lipid bicelles[32,44] suggested that the αIIb TM is perpendicular to the plane of the membrane (with an intracellular border at K994 for the isolated αIIb TM or at G991 in the presence of the β3 TM helix), whereas β3 is tilted ~25˚ relative to the normal axis of the membrane, resulting in an intracellular border[29,39] at D723. Recent experiments using environmentally-sensitive fluorophores at the inner or outer membrane-water interfaces of the isolated integrin β3 TM domain[19] suggested that binding of the FERM (four-point-one, ezrin, radixin, moesin) F3-F2 domains of talin to the β3 CT domain through the 744NPxY747 motif further enhanced tilting of the β3 TM domain, thus repositioning β3 I721 and L694 to a more hydrophobic environment. These findings were supported by multiscale MD simulations of incomplete forms of the integrin αIIbβ3 TM/CT helix dimer with or without talin.[25,26] Average tilt angles of ~5˚ for the αIIb TM helix and ~30˚ for the β3 TM helix were monitored during the multiscale simulations of the integrin αIIbβ3 TM/CT helix dimer without talin, although it must be noted that the αIIb TM helix was restrained to be perpendicular to the membrane during the relatively long, coarse-grained runs. Similar simulations carried out in the presence of talin revealed a significant increase in the β3 TM helix tilt angle of approximately 15˚ over the course of the simulation, relative to that observed in the multiscale simulations of the αIIbβ3 TM/CT domain without talin.[25,26]

In the large-scale, all-atom MD simulations reported here, no restraints were imposed on the orientation of the αIIb TM helix over the course of the simulation, although this helix was

initially placed perpendicular to the membrane, with the aforementioned experimentally-inferred borders extending into the lipid environment. Our all-atom, 3 μs MD simulations of the complete 2K9J-based αIIbβ3 TM/CT model structure revealed pronounced tilting of both β3 and αIIb helices in the lipid bilayer, with or without talin. Specifically, tilt angles increased to –40°±10° for the αIIb TM helix and to –44°±10° for the β3 helix during simulations without talin (black lines in Fig. 2B and 2C, respectively). During the 5 μs simulations conducted in the presence of talin, these angles stabilized at –37°±10° and –35°±10° for αIIb and β3, respectively (red lines in Fig. 2B and 2C, respectively), thus positioning αIIb I964-P965 residues into a more hydrophobic environment, and further embedding residues at the intracellular end of αIIb and β3 into the membrane (see Fig. S5). These results are in agreement with the suggested intracellular borders of the integrin active state at αIIb P998 and β3 F727 based on the results of a very recent analysis of intact αIIbβ3 in living cells using the substituted cysteine scanning accessibility method (SCSAM).[24]. This analysis suggests a more pronounced activation-driven tilting of both αIIb and β3 subunits than that previously inferred. Specifically, the αIIb helix border was shown to shift from the previously suggested K994 in the isolated αIIb[32] or G991 in the αIIbβ3 TM construct[29] to P998 because of a possible pulling of the extended ECD, and consequent embedding of the αIIb 994KRNRP998 stretch in the lipid bilayer. Similarly, the TM border of the β3 TM domain was found to extend from the previously inferred D723 for the isolated β3 subunit to E726 in intact αIIbβ3, suggesting a more pronounced activation-driven tilting of β3 for a more physiologically-relevant system.

In search of the molecular determinants that are responsible for the integrin inside-out signaling mechanism.

The 5 μs all-atom MD simulations of the complete 2K9J-based αIIbβ3 TM/CT model structure in the presence of talin-1 presented herein suggest novel, testable hypotheses of stable interactions between the αIIbβ3 TM/CT domain and talin-1 that may be worthy of experimental investigation in search of the molecular determinants that are responsible for the integrin inside-out signaling mechanism. Specifically, these interactions are: αIIb R997-talin E342, αIIb E1002-talin K316, αIIb E1005-talin K364, β3 T753-talin N355, β3 F754-talin Y373 and β3 R760-talin E293 (see interactions in Fig. 3A, 3B and their time evolution in Fig. S6). Notably, the simulated FERM subdomains of talin, i.e., F2-F3, undergo a major reorientation upon binding to both the β3 subunit and the membrane. Although the overall folds of the two subdomains remain mostly intact during simulation (RMSD of 2.9±0.42 and 1.4±0.25 Å for F2 and F3 domains, respectively), the F2 domain RMSD changes approximately 25.67±1.03 Å with respect to F3 (see inset in Fig. 3 and Fig. S7). This incidentally allows the F2 domain to establish a stable interaction between a positively charged patch composed of residues K263, K268, K272, K274, and K278 and the membrane (see Fig. 3C and Fig. S7), notwithstanding the lack of anionic lipids in the simplified membrane mimetic used in these simulations. Such anionic lipids have been reported to increase the interaction of talin with membranes.[31] Notably, the predicted orientation of talin-2 with respect to the membrane in the talin2/β1D structure[31] exhibited equivalent positions for the residues of the talin-2 charged patch. Unlike the ~5 μs all-atom simulations reported herein, recent ~1.5 μs coarse-grained simulations[28] failed to see association between talin and the zwitterionic POPC lipid, raising the question as to whether the missed association depends on the choice of the force field or the simulation length. On the other hand, a reorientation of F2 with respect to F3, which is made possible by a very flexible linker between them, was also observed as a result of the serial multiscale simulations.[26,28] We also note that

talin has been reported to activate purified αIIbβ3 in the absence of anionic phospholipids, namely, when embedded in neutral lipid nanodiscs[5] and when immune-captured to microtiter wells.[41]

The simulations reported here also suggest hypotheses of interaction changes between the F2 and F3 subdomains of talin-1 that occur upon F2 domain reorientation prior to anchoring itself to the membrane. Specifically, newly formed interactions during dynamics (Figure 3D) are: F3 E270-F2 K158, F3 E274-F2 K224, F3 E259-F2 R131, and F3 K328-F2 D132. In contrast, the F3 K269-F2 E193 interaction, which is present in the initial structure based on the homology model of the murine talin-2, is lost during simulation. We propose that engineering cysteine mutations at the positions involved in this latter interaction may prevent the positively charged patch of F2 from reaching the membrane, thus interfering with the process of integrin activation. Finally, the simulations reported here suggest stable interactions between talin-1 and the complete β3 CT, which exhibited a disordered, and hence unresolved, segment in the crystal structure of the β1D CT with murine talin-2. Specifically, these interactions are: β3 T753/talin N355, β3 F754/talin Y373 and β3 R760/talin E293 (Fig. S6). Notably, the 756NPXY759 motif of the β3 CT, which has been suggested to interact with kindlin, remains exposed to a possible interaction with this protein.

All-atom, long-scale MD simulations support a mechanisms of inside-out signaling that does not require helix separation.

Three different mechanisms have been proposed in the literature to explain how talin can trigger αIIbβ3 activation. The first one, which is supported by several *in vitro* studies (see [4] for a recent review), entails disruptions at both OMC and IMC induced by tilting, pistoning, and/or

lateral motions of the β3 subunit upon its direct interaction with the F3 subdomain of talin. This interaction is sufficient to induce integrin activation,[45] notwithstanding other potentially important interactions between a positively charged patch of the talin F2 domain and the membrane.[31] The favorable surface interaction between talin and the phospholipid bilayer has been proposed to dominate the ternary interaction involving talin-1 and the β3 CT domain.[20] The second hypothesis, supported by structural information,[31] relies on a possible competition between talin K324 and αIIb R995 in its interaction with β3 D723, thus favoring destabilization of the integrin low-affinity state. Finally, a third hypothesis attributes integrin activation to an interface disruption between the integrin α and β subunits due to talin-induced steric hindrance.[6] Multiscale MD simulations[25,26,28] have supported the first of these proposed mechanisms, although inferences were based on all-atom MD simulations of only up to 100 ns following approximate, coarse-grained simulations of αIIbβ3 constructs containing partial CTs. Recent all-atom MD simulations[27] of a full-length integrin αIIbβ3 model composed of the αIIbβ3 ECD (PDBid: 3FCS[2]) and the CD3CN/H2O NMR structure of the αIIbβ3 TM and CT domains (2KNC[21]) in complex with talin also support the hypothesis that talin's interaction with the membrane-proximal and membrane-distal regions of the αIIbβ3 TM and CT domains significantly loosens the IMC based on conclusions drawn from relatively short, pulling simulations. Experimentally, the role of talin in the mechanism of integrin inside-out activation appears to be further complicated by the presence in the cell of other important integrin regulators such as kindlin, which is known to interact through its F3 domain with the β3 membrane distal 756NPXY759 motif.[46,47]

The simultaneous tilting of the αIIb and β3 TM helices relative to the normal axis of the membrane resulting from our 5 μs simulations of the restraint-free, all-atom complex formed by

the αIIbβ3 TM/CT and F2-F3 talin domains prevents a drastic change in the right-handed crossing angle (–35°±8° in the presence of talin compared to –33°±8° in its absence; see red and black lines, respectively, in Fig. 2A) and/or the 'scissoring' motion observed in the recent coarse-grained simulations of the αIIbβ3 TM/CT domain where the αIIb TM helix had been restrained to be perpendicular to the membrane plane.[26] In contrast to the hypothesis that talin binding induces IMC and OMC disruption within the αIIbβ3 TM/CT system through helix separation,[48] hinging/scissors,[26,28,49] and/or piston-like[49] motions, none of these motions appeared to be significant during the simulations presented herein. This result is in agreement with the proposed lack of TM separation upon integrin activation from recent studies of intact αIIbβ3 using solution X-ray scattering and electron microscopy as well as the studies of talin-induced activation of intact αIIbβ3 in a nanodisc.[18] These latter studies are consistent with our findings that the interaction of the talin F2-F3 domains with the αIIbβ3 TM/CT protein portion did not disrupt the salt-bridge between αIIb R995 and β3 D723 (red line in Fig. 4A) and the failure of our data to support the proposed competition between talin-1 K324 and αIIb R995 for binding to β3 D723[31] as a basis for IMC destabilization. In contrast, the three residues are involved in a network of stable interactions that are maintained during the entire simulated timescale. Notably, while a stable interaction is formed between the β3 K716 side chain and the αIIb F992/K994 backbone carbonyl oxygens (black lines in Fig. 4B and 4C, respectively) during the 3 μs of the αIIbβ3 TM/CT domain simulated without talin, the latter interaction is lost in the 5 μs simulation with talin (red line in Fig. 4C) as αIIb F992 is displaced from its position at the interface between α and β. This appears to be the result of a slight rotation of one helix with respect to the other, which we propose may contribute to the long-range conformational changes leading to integrin activation. As a rough indication of this motion, we note that the difference between the rotation

angles of each TM segment around its axis, $\Delta\omega=\omega(\alpha IIb)-\omega(\beta 3)$, is roughly zero for the simulation in the absence of talin (Fig. S9C, black curve), while its average is as big as -25° in the presence of talin (Fig. S9C, red curve).

A destabilization of the IMC in the conformation stabilized by talin binding is evident from interaction energies between residues involved in inter-helical interactions. Specifically, we calculated the total dispersion and electrostatics interaction between residues M987/F992/F993 in αIIb and L712/W715/K716/I719 in β3. In the absence of talin, the IMC contributes ~12 kJ/mol (i.e., 5kT) to the overall ~75 kJ/mol stabilization enthalpy. The time-dependence of these energies is reported with black lines in Fig. S10 (plots in panel A and panel C correspond to the IMC and total energies, respectively). When talin is bound, the IMC contribution becomes marginal, thus reducing the overall inter-helix interaction to ~59 kJ/mol (red curves in panels A and C of Fig. S10). In contrast, no appreciable difference is observed in the interactions comprising the OMC (defined as residues G972/G976/L979/L980 in αIIb and V700/M701/I704/L705/G708 in β3) and the contribution of the OMC to the inter-helix enthalpy is constant throughout the simulation. Although our simulations cannot rule out changes in the overall free-energy of the OMC, the presence of talin does not seem to materially affect its conformation (see Fig. S10B).

Whether the slight IMC destabilization observed upon talin binding in these first large-scale, all-atom MD simulations of the complete αIIbβ3 TM/CT domain is sufficient to initiate the long-range conformational changes associated with integrin activation or constitutes the first of multiple steps leading to helix separation, is difficult to ascertain unambiguously based on these simulations, and requires further exploration. Indeed we cannot exclude the possibility that the

herein reported atomistic simulations are still limited in length, notwithstanding the multi-microsecond scale explored.

ACKNOWLEDGMENTS

Computations were supported in part through the computational resources and staff expertise provided by the Scientific Computing Facility at the Icahn School of Medicine at Mount Sinai, in part on TeraGrid advanced computing resources provided by Texas Advanced Computing Center through MCB080077, and in part on Anton at NRBSC/PSC through MCB110024P.

REFERENCES

1. Coller BS, Shattil SJ. The GPIIb/IIIa (integrin alphaIIbbeta3) odyssey: a technology-driven saga of a receptor with twists, turns, and even a bend. Blood 2008;112(8):3011-3025.
2. Zhu J, Luo BH, Xiao T, Zhang C, Nishida N, Springer TA. Structure of a complete integrin ectodomain in a physiologic resting state and activation and deactivation by applied forces. Mol Cell 2008;32(6):849-861.
3. Hynes RO. Integrins: bidirectional, allosteric signaling machines. Cell 2002;110(6):673-687.
4. Hu P, Luo BH. Integrin bi-directional signaling across the plasma membrane. J Cell Physiol 2013;228(2):306-312.
5. Ye F, Hu G, Taylor D, Ratnikov B, Bobkov AA, McLean MA, Sligar SG, Taylor KA, Ginsberg MH. Recreation of the terminal events in physiological integrin activation. J Cell Biol 2010;188(1):157-173.
6. Ye F, Kim C, Ginsberg MH. Molecular mechanism of inside-out integrin regulation. J Thromb Haemost 2011;9 Suppl 1:20-25.
7. Shattil SJ, Kim C, Ginsberg MH. The final steps of integrin activation: the end game. Nat Rev Mol Cell Biol 2010;11(4):288-300.
8. Takagi J, Petre BM, Walz T, Springer TA. Global conformational rearrangements in integrin extracellular domains in outside-in and inside-out signaling. Cell 2002;110(5):599-511.
9. Luo BH, Carman CV, Springer TA. Structural basis of integrin regulation and signaling. Annu Rev Immunol 2007;25:619-647.

10. Kim C, Lau TL, Ulmer TS, Ginsberg MH. Interactions of platelet integrin alphaIIb and beta3 transmembrane domains in mammalian cell membranes and their role in integrin activation. Blood 2009;113(19):4747-4753.

11. Li W, Metcalf DG, Gorelik R, Li R, Mitra N, Nanda V, Law PB, Lear JD, Degrado WF, Bennett JS. A push-pull mechanism for regulating integrin function. Proc Natl Acad Sci U S A 2005;102(5):1424-1429.

12. Luo BH, Carman CV, Takagi J, Springer TA. Disrupting integrin transmembrane domain heterodimerization increases ligand binding affinity, not valency or clustering. Proc Natl Acad Sci U S A 2005;102(10):3679-3684.

13. Luo BH, Springer TA, Takagi J. A specific interface between integrin transmembrane helices and affinity for ligand. PLoS Biol 2004;2(6):e153.

14. Partridge AW, Liu S, Kim S, Bowie JU, Ginsberg MH. Transmembrane domain helix packing stabilizes integrin alphaIIbbeta3 in the low affinity state. J Biol Chem 2005;280(8):7294-7300.

15. Wang W, Zhu J, Springer TA, Luo BH. Tests of integrin transmembrane domain homo-oligomerization during integrin ligand binding and signaling. J Biol Chem 2011;286(3):1860-1867.

16. Yin H, Slusky JS, Berger BW, Walters RS, Vilaire G, Litvinov RI, Lear JD, Caputo GA, Bennett JS, DeGrado WF. Computational design of peptides that target transmembrane helices. Science 2007;315(5820):1817-1822.

17. Zhu J, Carman CV, Kim M, Shimaoka M, Springer TA, Luo BH. Requirement of alpha and beta subunit transmembrane helix separation for integrin outside-in signaling. Blood 2007;110(7):2475-2483.

18. Eng ET, Smagghe BJ, Walz T, Springer TA. Intact alphaIIbbeta3 integrin is extended after activation as measured by solution X-ray scattering and electron microscopy. J Biol Chem 2011;286(40):35218-35226.

19. Kim C, Ye F, Hu X, Ginsberg MH. Talin activates integrins by altering the topology of the beta transmembrane domain. J Cell Biol 2012;197(5):605-611.

20. Moore DT, Nygren P, Jo H, Boesze-Battaglia K, Bennett JS, DeGrado WF. Affinity of talin-1 for the beta3-integrin cytosolic domain is modulated by its phospholipid bilayer environment. Proc Natl Acad Sci U S A 2012;109(3):793-798.

21. Yang J, Ma YQ, Page RC, Misra S, Plow EF, Qin J. Structure of an integrin alphaIIb beta3 transmembrane-cytoplasmic heterocomplex provides insight into integrin activation. Proc Natl Acad Sci U S A 2009;106(42):17729-17734.

22. Metcalf DG, Moore DT, Wu Y, Kielec JM, Molnar K, Valentine KG, Wand AJ, Bennett JS, DeGrado WF. NMR analysis of the alphaIIb beta3 cytoplasmic interaction suggests a mechanism for integrin regulation. Proc Natl Acad Sci U S A 2010;107(52):22481-22486.

23. Kahner BN, Kato H, Banno A, Ginsberg MH, Shattil SJ, Ye F. Kindlins, integrin activation and the regulation of talin recruitment to alphaIIbbeta3. PLoS One 2012;7(3):e34056.

24. Kurtz L, Kao L, Newman D, Kurtz I, Zhu Q. Integrin alphaIIbbeta3 inside-out activation: an in situ conformational analysis reveals a new mechanism. J Biol Chem 2012;287(27):23255-23265.

25. Kalli AC, Wegener KL, Goult BT, Anthis NJ, Campbell ID, Sansom MS. The structure of the talin/integrin complex at a lipid bilayer: an NMR and MD simulation study. Structure 2010;18(10):1280-1288.

26. Kalli AC, Campbell ID, Sansom MS. Multiscale simulations suggest a mechanism for integrin inside-out activation. Proc Natl Acad Sci U S A 2011;108(29):11890-11895.

27. Mehrbod M, Trisno S, Mofrad MR. On the Activation of Integrin alphaIIbbeta3: Outside-in and Inside-out Pathways. Biophys J 2013;105(6):1304-1315.

28. Kalli AC, Campbell ID, Sansom MS. Conformational changes in talin on binding to anionic phospholipid membranes facilitate signaling by integrin transmembrane helices. PLoS Comput Biol 2013;9(10):e1003316.

29. Lau TL, Kim C, Ginsberg MH, Ulmer TS. The structure of the integrin alphaIIbbeta3 transmembrane complex explains integrin transmembrane signalling. EMBO J 2009;28(9):1351-1361.

30. Shaw DE, Deneroff MM, Dror RO, Kuskin JS, Larson RH, Salmon JK, Young C, Batson B, Bowers KJ, Chao JC, Eastwood MP, Gagliardo J, Grossman JP, Ho CR, Ierardi DJ, Kolossvary I, Klepeis JL, Layman T, McLeavey C, Moraes MA, Mueller R, Priest EC, Shan YB, Spengler J, Theobald M, Towles B, Wang SC. Anton, a special-purpose machine for molecular dynamics simulation. Communications of the Acm 2008;51(7):91-97.

31. Anthis NJ, Wegener KL, Ye F, Kim C, Goult BT, Lowe ED, Vakonakis I, Bate N, Critchley DR, Ginsberg MH, Campbell ID. The structure of an integrin/talin complex reveals the basis of inside-out signal transduction. EMBO J 2009;28(22):3623-3632.

32. Lau TL, Dua V, Ulmer TS. Structure of the integrin alphaIIb transmembrane segment. J Biol Chem 2008;283(23):16162-16168.

33. Mackerell Jr. AD, Bashford D, Bellot M, Dunbrack RL, Evanseck JD, Field MJ, Fischer S, Gao J, Guo H, Ha S, Joseph-McCarthy D, Kuchnir L, Kuczera K, Lau TK, Mattos C, Michnick S, Ngo T, Nguyen DT, Prodhom B, Reiher WE, Roux B, Schlenkrich B, Smith J, Stote R, Straub J, Watanabe M, Wiorkiewicz-Kuczera J, Karplus M. All-atom empirical potential for molecular modeling and dynamics studies of proteins. J Phys Chem B 1998;102:3586-3616.

34. Mackerell AD, Jr., Feig M, Brooks CL, 3rd. Extending the treatment of backbone energetics in protein force fields: limitations of gas-phase quantum mechanics in reproducing protein conformational distributions in molecular dynamics simulations. J Comput Chem 2004;25(11):1400-1415.

35. Mezei M, Filizola M. TRAJELIX: a computational tool for the geometric characterization of protein helices during molecular dynamics simulations. J Comput Aided Mol Des 2006;20(2):97-107.

36. Mezei M. Simulaid: A simulation facilitator and analysis program. Journal of Computational Chemistry 2010;31(14):2658–2668.

37. Barth P, Schonbrun J, Baker D. Toward high-resolution prediction and design of transmembrane helical protein structures. Proc Natl Acad Sci U S A 2007;104(40):15682-15687.

38. Barth P, Wallner B, Baker D. Prediction of membrane protein structures with complex topologies using limited constraints. Proc Natl Acad Sci U S A 2009;106(5):1409-1414.

39. Zhu J, Luo BH, Barth P, Schonbrun J, Baker D, Springer TA. The structure of a receptor with two associating transmembrane domains on the cell surface: integrin alphaIIbbeta3. Mol Cell 2009;34(2):234-249.

40. Hughes PE, Diaz-Gonzalez F, Leong L, Wu C, McDonald JA, Shattil SJ, Ginsberg MH. Breaking the integrin hinge. A defined structural constraint regulates integrin signaling. J Biol Chem 1996;271(12):6571-6574.

41. Vinogradova O, Velyvis A, Velyviene A, Hu B, Haas T, Plow E, Qin J. A structural mechanism of integrin alpha(IIb)beta(3) "inside-out" activation as regulated by its cytoplasmic face. Cell 2002;110(5):587-597.

42. Armulik A, Nilsson I, von Heijne G, Johansson S. Determination of the border between the transmembrane and cytoplasmic domains of human integrin subunits. J Biol Chem 1999;274(52):37030-37034.

43. Stefansson A, Armulik A, Nilsson I, von Heijne G, Johansson S. Determination of N- and C-terminal borders of the transmembrane domain of integrin subunits. J Biol Chem 2004;279(20):21200-21205.

44. Lau TL, Partridge AW, Ginsberg MH, Ulmer TS. Structure of the integrin beta3 transmembrane segment in phospholipid bicelles and detergent micelles. Biochemistry 2008;47(13):4008-4016.

45. Calderwood DA, Yan B, de Pereda JM, Alvarez BG, Fujioka Y, Liddington RC, Ginsberg MH. The phosphotyrosine binding-like domain of talin activates integrins. J Biol Chem 2002;277(24):21749-21758.

46. Moser M, Nieswandt B, Ussar S, Pozgajova M, Fassler R. Kindlin-3 is essential for integrin activation and platelet aggregation. Nat Med 2008;14(3):325-330.

47. Harburger DS, Bouaouina M, Calderwood DA. Kindlin-1 and -2 directly bind the C-terminal region of beta integrin cytoplasmic tails and exert integrin-specific activation effects. J Biol Chem 2009;284(17):11485-11497.

48. Kim M, Carman CV, Springer TA. Bidirectional transmembrane signaling by cytoplasmic domain separation in integrins. Science 2003;301(5640):1720-1725.

49. Williams MJ, Hughes PE, O'Toole TE, Ginsberg MH. The inner world of cell adhesion: integrin cytoplasmic domains. Trends Cell Biol 1994;4(4):109-112.

Figure Legends

Figure 1. Complete αIIbβ3 TM/CT models based on: (A) NMR structure of complete integrin αIIbβ3 TM and CT domains in a CD3CN/H2O mixture (PDBid: 2KNC) and (B) NMR structure of the same complex with truncated CT domains in phospholipid bicelles (PDB: 2K9J). Details of the Outer Membrane Clasp (OMC) and the Inner Membrane Clasp (IMC) are shown in panels C, D or E, F for models depicted in A and B, respectively. In all panels, the αIIb and β3 subunits are shown in blue and red, respectively.

Figure 2. Time evolution of crossing (A) and tilting angles of αIIb (B) and β3 (C) TM helices in the 2K9J-based models simulated in the presence (red line) or absence (black line) of talin-1 F2 and F3 domains.

Figure 3. Representative snapshot of the 5μs MD simulations of the complete αIIbβ3 TM/CT/talin model. Novel interactions observed during simulation (A) between residues of the αIIb TM (in blue) and the F3 domain of talin-1 (in dark green), specifically: αIIb R997-talin E342, αIIb E1002-talin K316, αIIb E1005-talin K364, and (B) between residues of the β3 TM (in red) and the F3 domain of talin-1 (β3 T753-talin N355, β3 F754-talin Y373 and β3 R760-talin E293)**.** (C) Details of the interactions between the positively charged patch of the F2 domain of talin-1 (in light green) and the membrane. The inset shows the rotation of the F2 domain with respect to F3 during the 5 μs MD simulations.

Figure 4. Selected electrostatic interactions between αIIb and β3 TM residues located at the IMC. These interactions are: (A) αIIb R995/β3 D723 (ionic lock), (B) αIIb F992/β3 K726 and (C) αIIb K994/β3 K716. The red and black lines indicate the time evolution of these interactions in the 2K9J-based system simulated with or without talin-1 F2 and F3 domains, respectively.

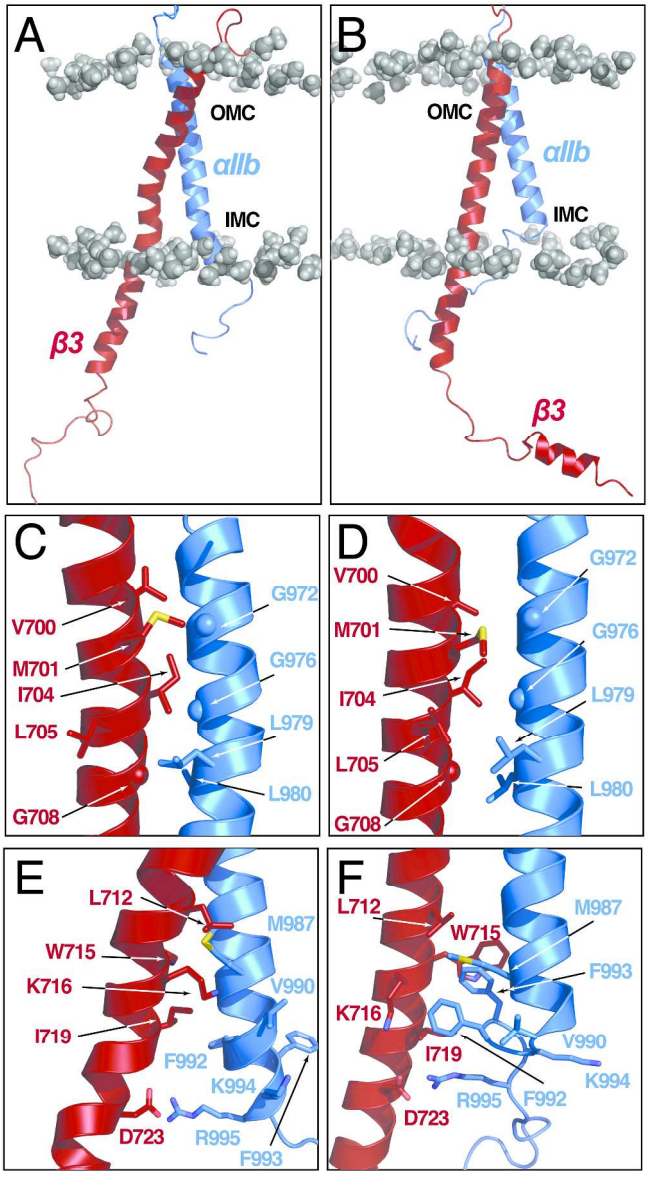

Figure 1. Complete αIIbβ3 TM/CT models based on: (A) NMR structure of complete integrin αIIbβ3 TM and CT domains in a CD3CN/H2O mixture (PDBid: 2KNC) and (B) NMR structure of the same complex with truncated CT domains in phospholipid bicelles (PDB: 2K9J). Details of the Outer Membrane Clasp (OMC) and the Inner Membrane Clasp (IMC) are shown in panels C, D or E, F for models depicted in A and B, respectively. In all panels, the αIIb and β3 subunits are shown in blue and red, respectively.
265x459mm (300 x 300 DPI)

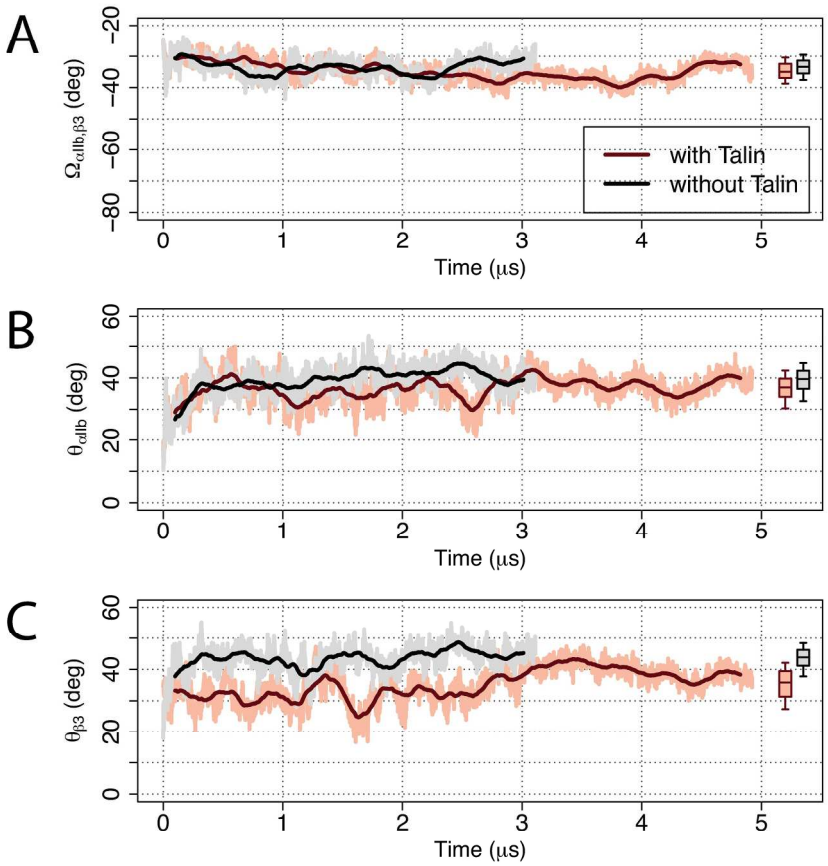

Figure 2. Time evolution of crossing (A) and tilting angles of αIIb (B) and β3 (C) TM helices in the 2K9J-based models simulated in the presence (red line) or absence (black line) of talin-1 F2 and F3 domains.
207x204mm (300 x 300 DPI)

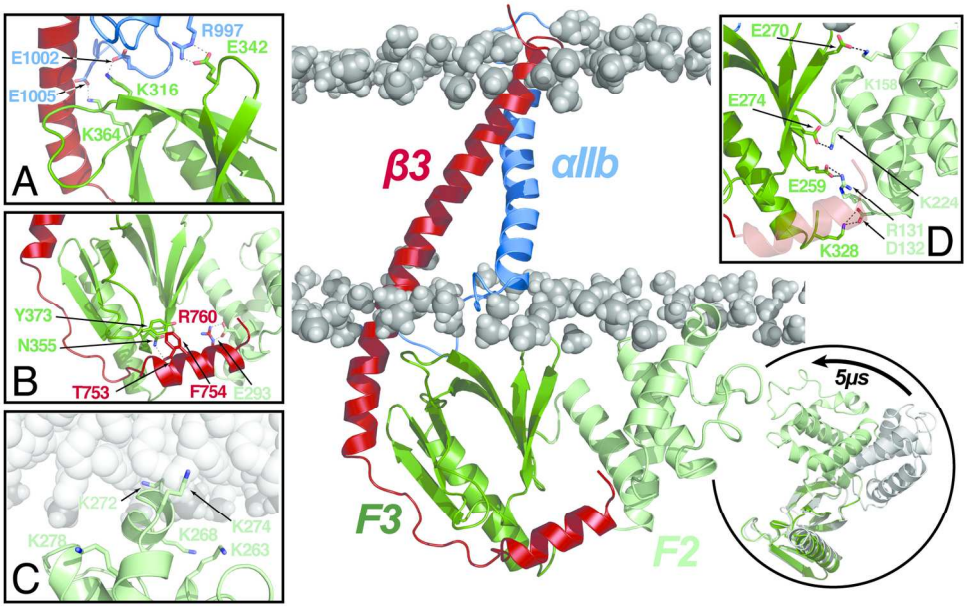

Figure 3. Representative snapshot of the 5μs MD simulations of the complete αIIbβ3 TM/CT/talin model. Novel interactions observed during simulation (A) between residues of the αIIb TM (in blue) and the F3 domain of talin-1 (in dark green), specifically: αIIb R997-talin E342, αIIb E1002-talin K316, αIIb E1005-talin K364, and (B) between residues of the β3 TM (in red) and the F3 domain of talin-1 (β3 T753-talin N355, β3 F754-talin Y373 and β3 R760-talin E293). (C) Details of the interactions between the positively charged patch of the F2 domain of talin-1 (in light green) and the membrane. The inset shows the rotation of the F2 domain with respect to F3 during the 5 μs MD simulations.
161x101mm (300 x 300 DPI)

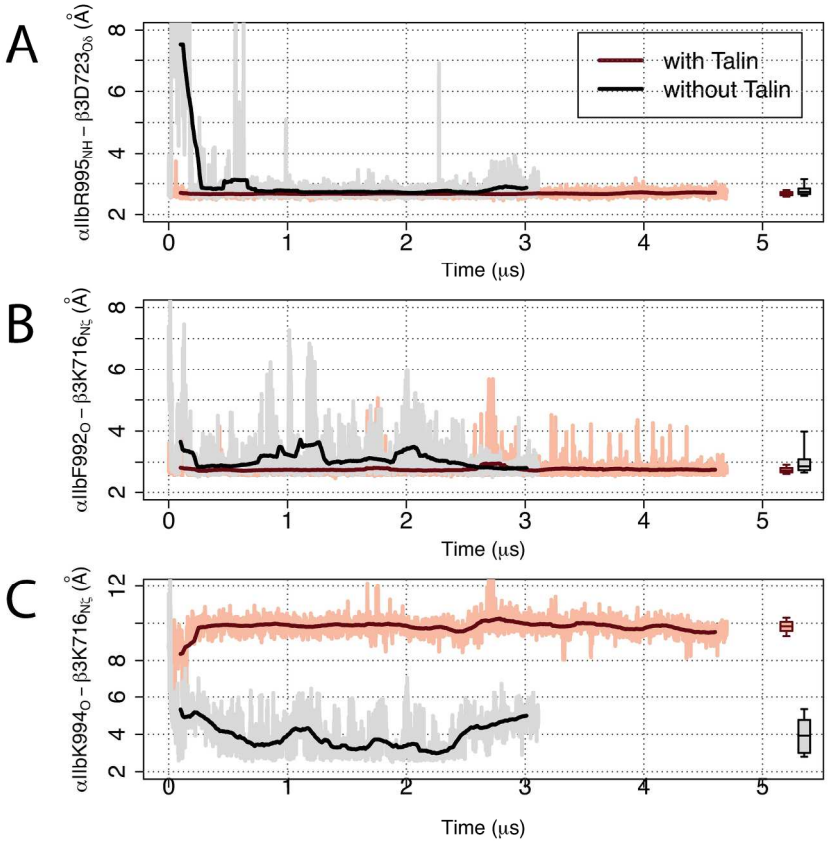

Figure 4. Selected electrostatic interactions between αIIb and β3 TM residues located at the IMC. These interactions are: (A) αIIb R995/β3 D723 (ionic lock), (B) αIIb F992/β3 K726 and (C) αIIb K994/β3 K716. The red and black lines indicate the time evolution of these interactions in the 2K9J-based system simulated with or without talin-1 F2 and F3 domains, respectively.
204x196mm (300 x 300 DPI)